16th World Conference on Earthquake, 16WCEE 2017

Santiago Chile, January 9th to 13th 2017

Paper N° 1265

Registration Code: S-XXXXXXXX

FEASIBLITY OF VISCOUS MASS DAMPER WITH BINGHAM FLUID ORIGINED FORCE RESTRICTION MECHANISM FOR BASE-ISOLATED STRUCTURE

M. Ikenaga[(1)], K. Ikago[(2)], N. Inoue[(3)]

[(1)] *Associate Professor, Dept. of Architecture, Faculty of Environmental and Urban Engineering, Kansai University,mikenaga@kansai-u.ac.jp*
[(2)] *Professor, International Research Institute of Disaster Science, Tohoku University, ikago@irides.tohoku.ac.jp*
[(3)] *Professor emeritus, Tohoku University, norio8norio@gmail.com*

Abstract

Viscous mass dampers with friction origin force restriction mechanism (force restricted viscous mass damper, hereinafter called FRVMD) are considered for base isolated structures. From a series of analytical studies, FRVMD can reduce the displacement of the base isolation layer, but they cannot reduce the floor response acceleration of the superstructure depending on the input ground motions. To improve the damper, viscous mass dampers with Bingham fluid origin force restriction (Bingham fluid – viscous mass damper, hereinafter called BF-VMD) is suggested.

The BF-VMD has four design variables to be determined, the amount of the apparent mass, the viscous damping coefficient, the stiffness of buffer spring, and the damping coefficient of the Bingham fluid. In this paper, base isolated five-story reinforced concrete structure incorporated with BF-VMD, FRVMD, or ordinary oil dampers with relief mechanism (hereinafter called OD) at the base isolation layer are considered as a common isolated structure. Three kinds of design criteria that are the displacement of the base isolation layer, the floor response acceleration, and the coefficient of the shear force, are defined for three levels of input ground motions, and the design variables that can fulfill all the design criteria are chosen by the optimum design method.

The maximum responses given by the optimization results show that the structure with optimized BF-VMD can satisfy all the design criteria, whereas the structure with FRVMD or OD cannot satisfy the design criteria of the floor response acceleration. The response magnification of the floor response acceleration shows that the high frequency component of the floor response acceleration in case of BF-VMD becomes smaller than that in case of FRVMD. We infer that this is because of the difference of the mechanism on the force restriction.

Keywords: Base isolation, Viscous mass damper, Optimum design method, Force restriction

1. Introduction

The apparent mass which generates the inertial force according to the relative acceleration of two nodes is called the inerter [1]. Recently because of the implementation of this inerter, many seismic control studies have been performed using this kind of device. Furuhashi and Ishimaru et al. [2-5] use inerter devices to control the structure mode shape. Isoda et al. [6-9] investigated the characteristics of the input energy from the seismic excitation due to the inerter. Sugimura and Saito [10-12] develop a tuned mass damper-like device designated the tuned viscous mass damper by connecting an inerter with soft supporting spring. Wang et al. [13] consider the frequency response characteristics for various configurations of the inerter, damping element, and supporting spring. The inerter in these research works are basically employed in the seismic control structure to reduce the response displacement under seismic excitation.

On the other hand, Nakaminami et al. [14] install the viscous mass damper which constitutes the inerter and the viscos element in parallel configuration to achieve the response control for base isolated structure. In case of the base isolated structure, it is necessarily to reduce the displacement of the isolation layer without the deterioration of isolation performance, i.e., an increase in floor response acceleration of the superstructure need to be restrained. Nakaminami et al. [15] propose the viscous mass damper with force restriction mechanism (hereinafter denoted as force restricted viscous mass damper, FRVMD) in which rotational friction is utilized to restrict excessive control forces so as to achieve better performance in reduction of floor response accelerations.

There are still five problems to be addressed for FRVMD; (1) The restricted force is constant because the force restriction is delivered by the friction force. (2) The damper behavior exhibits strong non-linearity due to low restriction force to maintain low floor response acceleration. (3) The damper design procedure to realize the effective damper for both megathrust earthquakes and near fault earthquakes becomes complicated because of the non-linearity. (4) The strong effect to reduce the displacement leads to an increase of response acceleration by some input ground motions. (5) The difficulty of managing the friction element for the force restriction mechanism.

Bingham fluid exhibits a hysteresis similar to a friction element. The performance of the Bingham fluid damper is reported by Takeuchi and Ikenaga [16] analytically and experimentally. It is indicated that the Bingham fluid has a stable properties with respect to environmental conditions such as temperature and velocity. We focused on these properties and proposed to replace the friction element with the Bingham fluid as a fluid clutch mechanism to control the damper force. It is expected that force restriction mechanism by the Bingham fluid can realize the maintenance-free and highly redundant system because of its properties. Ikenaga et al. [17] shows analytically the advantage of seismic control on base isolated structures by the viscous mass damper with Bingham fluid force restriction mechanism (hereinafter denoted as Bingham fluid viscous mass damper, BF-VMD). Figure 1 shows the overview of BF-VMD. The Bingham fluid that is enclosed between the rotational mass and the ball nut generates the viscous damping force instead of the friction material of FRVMD.

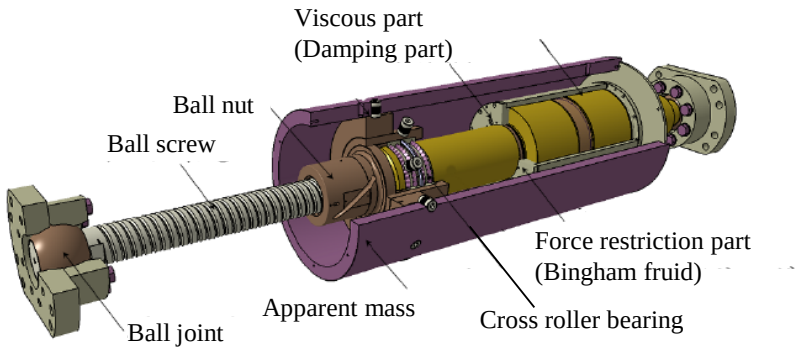

Fig. 1 Overview of BF-VMD

In general, the fixed point theory [18] is used to design the dynamic mass system. For example to design three design variables of the tuned viscous mass damper, which are amount of the apparent mass, the viscous coefficient, and the supporting spring, designers have to decide one variable in advance and the rest of the design variables are derived from the fixed point theory. It is shown that tuned viscous mass damper that is designed by the fixed point theory has a very good damping performance.

On the other hand, it is impossible to apply the fixed point theory to BF-VMD owing to the following two points. (1) The behavior of BF-VMD is non-linear. (2) The ratio of apparent mass to total mass should be large so that it is out of the scope of the application of the theory. Since BF-VMD has four design variables as described later, a large amount of parametric studies are necessary to determine the damper performance that can satisfy the several design criteria for multiple input ground motions.

The primary purpose of this study is to determine the design variables of BF-VMD which can satisfy the design criteria by the optimum design method [19]. Therefore another purpose is to compare the response of optimum designed BF-VMD with that of conventional oil damper with relief mechanism. The third purpose is to discuss the robustness of BF-VMD and the applicability to actual design.

2. Outline of Analytical study

2.1 Analysis model

In this study a base isolated 5-story reinforced concrete structure is considered as a benchmark analysis model. Figure 2 and Table 1 shows the analysis model and the basic characteristics. The base isolation layer is composed of natural rubber bearings, cross linear bearings, and lead rubber isolators to inhibit the vibration caused by the wind load. Lead rubber bearings shows the bi-linear behavior whose yielding share force coefficient is 0.02 and initial stiffness is 9 times as large as the stiffness of the isolation layer. The damping factor of superstructure is 2% of critical. One of the dampers, BF-VMD, FRVMD, and OD, is incorporated into the base isolation layer as the damping element for each case.

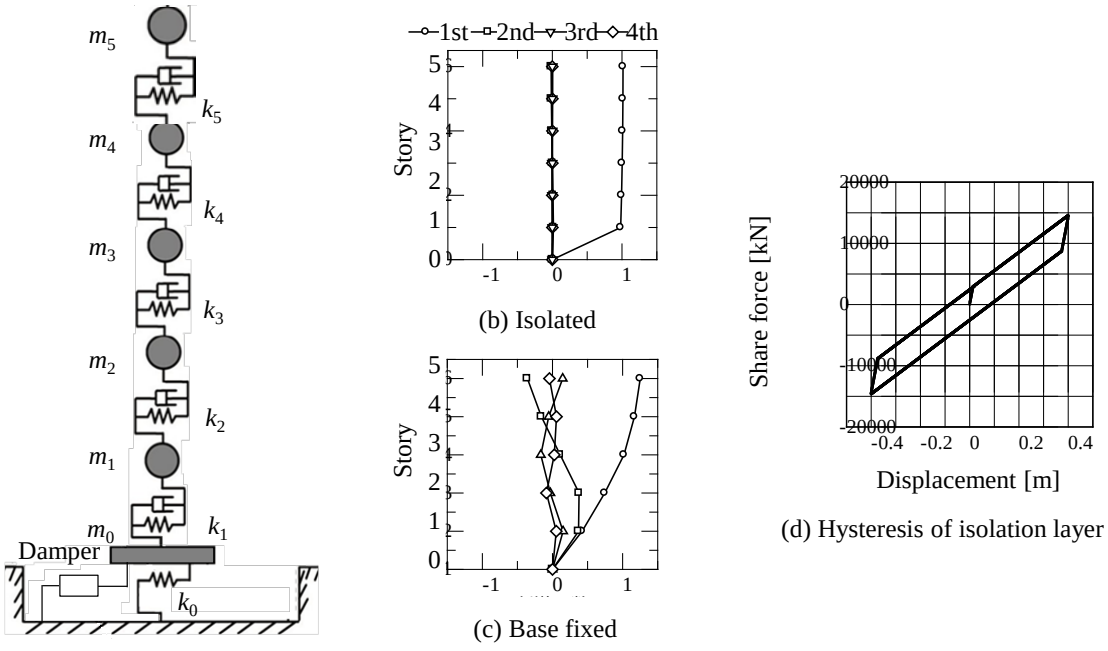

(a) Analysis model

(b) Isolated

(c) Base fixed

(d) Hysteresis of isolation layer

Fig.2 Analysis model

Table 1 Properties of analysis model

n	Story	Story hight [m]	Mass [ton]	Stiffness [kN/m]
5	5	3.80	1739	2290650
4	4	3.80	1800	2488300
3	3	4.40	1807	1938750
2	2	4.40	1928	2037850
1	1	5.45	2335	1759650
0	Base isolation layer	1.00	3057	31254
Sum		22.85	12666	-

Natural period [s]			
	1st	2nd	3rd
Base isolation (include LRI)	1.39	0.37	0.20
Base isolation (ignore LRI)	4.04	0.40	0.20
Base fixed	0.67	0.23	0.15

2.2 Definition of damper

Figure 3 illustrates analysis models of three dampers. x_0, x_b, x_r, and x_d are the isolator displacement, displacement of supporting spring, displacement of force restriction mechanism, and displacement of viscous damping element, respectively. The damping force of OD is defined as the force generated by the damping element, and those of FRVMD and BF-VMD are defined as the force generated by the supporting spring.

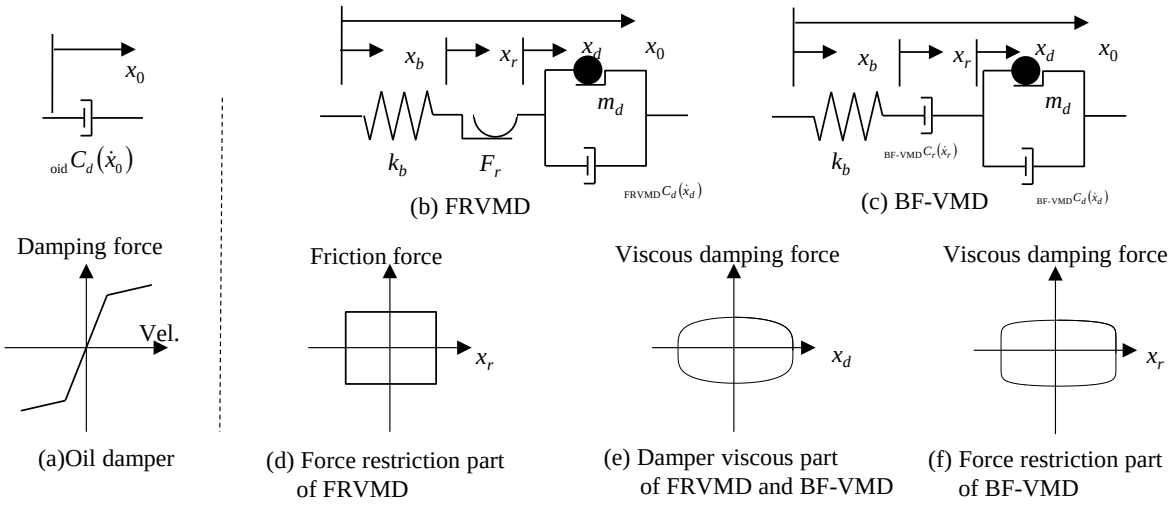

Fig.3 Analysis model of damper

A non-linearity of viscous damping element is also considered as shown in Figure 4. $_{\text{BF-VMD}}C_d(\dot{x}_d)$, $_{\text{FRVMD}}C_d(\dot{x}_d)$, and $_{\text{BF-VMD}}C_r(\dot{x}_r)$ are defined as the damping coefficient of BF-VMD damping part, the damping coefficient of FRVMD damping part, and the damping coefficient of BF-VMD force restriction part, respectively.

$$_{\text{BF-VMD}}C_d(\dot{x}_d) = {}_{\text{BF-VMD}}C_{cdv}|\dot{x}_d|^{\alpha_{cd}-1} \quad (\alpha_{cd}=0.50) \quad (1)$$

$$_{\text{FRVMD}}C_d(\dot{x}_d) = {}_{\text{FRVMD}}C_{cdv}|\dot{x}_d|^{\alpha_{cd}-1} \quad (\alpha_{cd}=0.50) \quad (2)$$

$$_{\text{BF-VMD}}C_r(\dot{x}_d) = {}_{\text{BF-VMD}}C_{crv}|\dot{x}_r|^{\alpha_{cr}-1} \quad (\alpha_{cr}=0.20) \quad (3)$$

Here, $_{\text{BF-VMD}}C_{cdv}$, $_{\text{FRVMD}}C_{cdv}$, and $_{\text{BF-VMD}}C_{crv}$ are the contant value for each damping part. Then each viscous damping force is given as follows:

$$_{\text{BF-VMD}}Q_{cd} = {}_{\text{BF-VMD}}C_{cdv}\left|\dot{x}_d\right|^{\alpha_{cd}-1}\dot{x}_d \quad (4)$$

$$_{\text{FRVMD}}Q_{cd} = {}_{\text{FRVMD}}C_{cdv}\left|\dot{x}_d\right|^{\alpha_{cd}-1}\dot{x}_d \quad (5)$$

$$_{\text{BF-VMD}}Q_{cr} = {}_{\text{BF-VMD}}C_{crv}\left|\dot{x}_r\right|^{\alpha_{cr}-1}\dot{x}_r \quad (6)$$

On the other hand, an OD is defined as a conventional oil damper with relief valve, whose damping coefficient and damping ratio are defined as Equations (7) and (8).

$$_{\text{oil}}C_d(\dot{x}_0) = \begin{cases} 2500\text{kNs/m} & (\dot{x}_0 \le 0.32\text{m/s}) \\ 800\text{kNs/m} & (\dot{x}_0 > 0.32\text{m/s}) \end{cases} \quad (7)$$

$$_{\text{oil}}h_d(\dot{x}_0) = \begin{cases} \dfrac{2500}{2\sqrt{k_0 m_{\text{total}}}} = 0.063 & (\dot{x}_0 \le 0.32\text{m/s}) \\ \dfrac{800}{2\sqrt{k_0 m_{\text{total}}}} = 0.201 & (\dot{x}_0 > 0.32\text{m/s}) \end{cases} \quad (8)$$

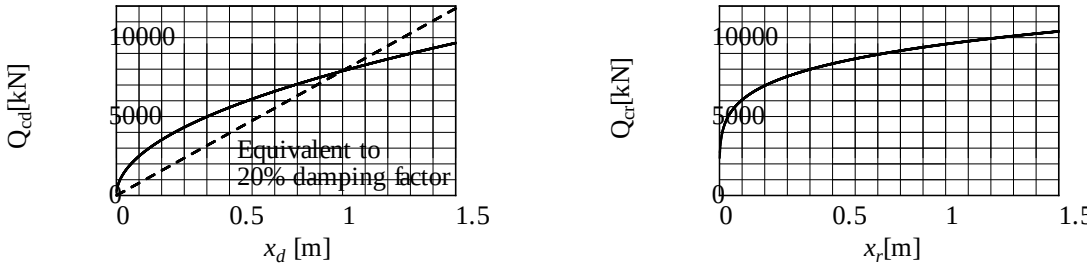

(a) Viscous damping part of BF-VMD and FRVMD (b) Force restriction part of BF-VMD

Fig. 4 Non-linearity of viscous elements

2.3 Definition of damper design variables

BF-VMD and FRVMD have four design variables each. As a common design variables, the ratio of the apparent mass to the total mass $\mu(=m_d/m_{total})$ and the frequency ratio of the additional system to the primary system $\beta(=\omega_d/\omega_0)$ are defined. Here m_{total} , ω_d, and ω_0 are the total mass of the structure, the frequency of the undamped additional system of BF-VMD and FRVMD, and the fundamental frequency of the undamped primary system, respectively. Three kinds of damping element which are the damping part of BF-VMD, damping part of FRVMD, and force restriction part of BF-VMD, are described as follows:

$$_{\text{BF-VMD}}\tilde{h}_d = \frac{{}_{\text{BF-VMD}}C_d(1\,[\text{m/s}])}{2\sqrt{k_0 m_{\text{total}}}} \quad (9)$$

$$_{\text{FRVMD}}\tilde{h}_d = \frac{{}_{\text{FRVMD}}C_d(1\,[\text{m/s}])}{2\sqrt{k_0 m_{\text{total}}}} \quad (10)$$

$$_{\text{BF-VMD}}\tilde{h}_r = \frac{{}_{\text{BF-VMD}}C_r(1\,[\text{m/s}])}{2\sqrt{k_0 m_{\text{total}}}} \quad (11)$$

where these damping coefficient are determined from the secant slope obtained from the damping force-velocity relationship at the velocity of 1m/s.

2.4 Formulation of analysis model

The equation of motion for this analysis model excited by a ground acceleration of x_g can be given as

$$M\ddot{X} + C\dot{X} + KX = -MI\ddot{x}_g \qquad (12)$$

$$M = \begin{bmatrix} m_0 & 0 & 0 & 0 & 0 & 0 \\ 0 & m_1 & 0 & 0 & 0 & 0 \\ 0 & 0 & \ddots & 0 & 0 & 0 \\ 0 & 0 & 0 & m_5 & 0 & 0 \\ 0 & 0 & 0 & 0 & m_d & 0 \\ 0 & 0 & 0 & 0 & 0 & 0 \end{bmatrix} \quad C = \begin{bmatrix} c_1 & -c_1 & 0 & 0 & 0 & 0 \\ -c_1 & c_1+c_2 & \ddots & 0 & 0 & 0 \\ 0 & \ddots & \ddots & -c_5 & 0 & 0 \\ 0 & 0 & -c_5 & c_5 & 0 & 0 \\ 0 & 0 & 0 & 0 & {}_{\mathrm{BF-VMD}}C_d & 0 \\ 0 & 0 & 0 & 0 & 0 & {}_{\mathrm{BF-VMD}}C_r \end{bmatrix} \quad K = \begin{bmatrix} k_0+k_1+k_b & -k_1 & 0 & 0 & -k_b & -k_b \\ -k_1 & k_1+k_2 & \ddots & 0 & 0 & 0 \\ 0 & \ddots & \ddots & -k_5 & 0 & 0 \\ 0 & 0 & -k_5 & k_5 & 0 & 0 \\ -k_b & 0 & 0 & 0 & k_b & k_b \\ -k_b & 0 & 0 & 0 & k_b & k_b \end{bmatrix}$$

$$X = \begin{bmatrix} x_0 & x_1 & x_2 & x_3 & x_4 & x_5 & x_d & x_r \end{bmatrix}^T$$

$$I = \begin{bmatrix} 1 & 1 & 1 & 1 & 1 & 1 & 0 & 0 \end{bmatrix}^T$$

The Newmark β method (β = 1/4) is used for time history analysis.

2.5 Input ground motion and design criteria

Twenty input ground motions listed in table 2 are applied in this study. These are classified into three levels depending on the peak ground velocity. Three kinds of maximum response limits are considered as design criteria (Table 3), (1) maximum displacement limit of the base isolation layer $D_{\max,\mathrm{No.}}$, (2) maximum floor response acceleration limit $A_{\max,\mathrm{No.}}$, (3) maximum story share force coefficient limit $R_{\max,\mathrm{No.}}$. Here No. denote the number of the input ground motion and $A_{\max,\mathrm{No.}}$ denotes the maximum floor response acceleration except the roof top acceleration because it is irrelevant to the habitability. Maximum response values of each input level is defined as

$$\begin{aligned} D_{\max,i} &= \max\left\{D_{\max,\mathrm{No.}}\right\} \\ A_{\max,i} &= \max\left\{A_{\max,\mathrm{No.}}\right\} \\ R_{\max,i} &= \max\left\{R_{\max,\mathrm{No.}}\right\} \end{aligned} \qquad \underline{i = \mathrm{Lv.1, Lv.2, Lv.3}} \quad \underline{\begin{cases} \mathrm{No.} = 1-5, \text{ when } i = \mathrm{Lv.1} \\ \mathrm{No.} = 6-14, \text{ when } i = \mathrm{Lv.2} \\ \mathrm{No.} = 15-20, \text{ when } i = \mathrm{Lv.3} \end{cases}} \qquad (13)$$

Table 2 List of input ground motion

Name	Notation	Level 1			Level 2			Level 3		
		No.	PGV [m/s]	PGA [m/s^2]	No.	PGV [m/s]	PGA [m/s^2]	No.	PGV [m/s]	PGA [m/s^2]
Imperial Valley, USA 1949	El-Centro	1		2.56	6		5.11	15		7.67
Hachinohe, Tokachi, Japan, 1968	Hachinohe	2		1.34	7		2.68	16		4.02
Kern County, USA, 1952	Taft	3	0.25	2.54	8	0.50	5.07	17	0.75	7.61
Tohoku Univ. Miyagi, Japan, 1978	Tohoku	4		1.71	9		3.41	18		5.12
JMA Kobe, Kobe, Japan, 1995	JMA-Kobe	5		2.49	10		4.98	19		7.47
Artificial wave of Sannomaru	Sannomaru				11	0.49	1.86			
Artificial wave (JMA-Kobe phase)	Art. Kobe				12	0.50	6.47			
Artificial wave (Taft phase)	Art. Taft				13	0.64	7.30			
Artificial wave (El-Centro phase)	Art. El-centro				14	0.61	4.87			
JR Takatori, Kobe, Japan, 1995	Takatori							20	1.27	6.57

Table 3 Design criteria

Input ground motion level i	Displacement of base isolation layer D_i [m]	Floor response acceleration A_i [m/s^2]	Coefficient of story share force R_i
Lv.1	0.10	1.50	0.20
Lv.2	0.25	2.50	0.20
Lv.3	0.45	2.50	0.20

2.6 Optimum design of damper

In reference to the previous research of FRVMD by Nakaminami et al., the mass ratio μ, the damping factor of damping part ${}_{\text{BF-VMD}}\tilde{h}_d$, and ${}_{\text{FRVMD}}\tilde{h}_d$ are fixed at 1.0, 0.2, and 0.2, respectively. Three other variables that are b, ${}_{\text{BF-VMD}}\tilde{h}_r$ for BF-VMD, and F_r for FRVMD are decided by the line search method that is one of the numerical optimization method. Optimum design problems for BF-VMD and FRVMD can be expressed as follows:

find $x = \{\beta,\ {}_{\text{BF-VMD}}\tilde{h}_r\}$

to minimize $A_{\max,Lv2.}$

subject to
$$D_{\max,i} \le D_i$$
$$A_{\max,i} \le A_i$$
$$R_{\max,i} \le R_i \quad (i\text{=Lv1,Lv2,Lv.3})$$
$$0.1 \le \beta \le 16.0$$
$$0.00 \le {}_{\text{BF-VMD}}\tilde{h}_r \le 0.50$$

find $x = \{\beta,\ F_r\}$

to minimize $A_{\max,Lv2.}$

subject to
$$D_{\max,i} \le D_i$$
$$A_{\max,i} \le A_i$$
$$R_{\max,i} \le R_i \quad (i\text{=Lv1,Lv2,Lv.3})$$
$$0.1 \le \beta \le 16.0$$

On the other hand, parametric study to decide the number of OD is conducted and the number which can minimise the maximum floor response acceleration for level 2 input ground motions is selected as the optimum number of OD.

3. Analysis Result

Figure 5 shows the maximum response results that are given by the optimally designed dampers. It is clear that only the BF-VMD can satisfy all the design criteria despite of that the maximum damping force is larger than those of other dampers. In contrast, FRVMD and OD cannot satisfy the design criteria on the maximum floor response acceleration that is closely related to the performance of base isolation.

Table 4 lists the optimum designs. The damping coefficient of the force restriction part is almost the same as that of damping part. This implies that the viscocity of the restriction part is almost the same as that of the viscous damping part and therefore it is expected that the damper mechanism shown in Figure 2 is feasible. Comparison on the damper parameters of BF-VMD with those of FRVMD shows that β of FRVMD is four times as large as that of FRVMD. Table 5 summarizes the input ground motions by which the maximum responses are yielded. As is evident from Table 5, BF-VMD can satisfy three design criteria for several kinds of input ground motions by the optimum design method.

It should be noted that these results are obtained in the range of the selected input ground motions listed in table 4. Although the result may change subject to the choice of input ground motions, we infer that four design variables of BF-VMD can assure the robustness of the optimum designs and feasible optimum design can be found even if the input ground motions are changed.

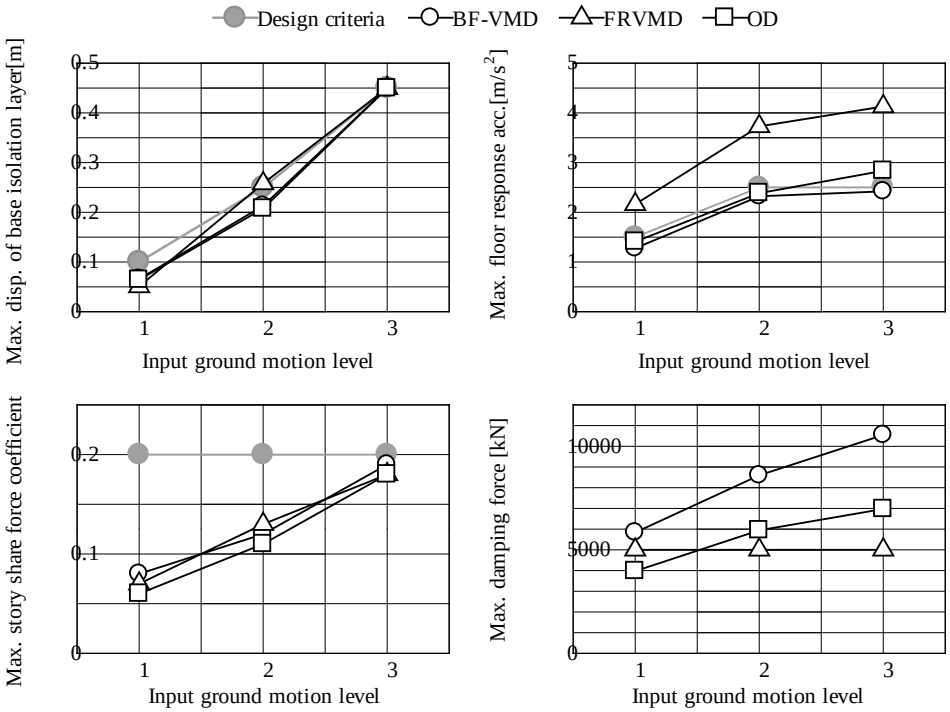

Fig. 5 Optimum designed analysis result

Table 4 Optimum property of damper

	Mass ratio	Damping part of damper	Force restriction part	Supporting spring
BF-VMD	μ=1.0	${}_{\mathrm{BF-VMD}}\tilde{h}_d = 20\%$	${}_{\mathrm{BF-VMD}}\tilde{h}_r = 24.0\%$	$\beta = 2.0$
FRVMD	μ=1.0	${}_{\mathrm{FRVMD}}\tilde{h}_d = 20\%$	$F_r = 5000\mathrm{kN}$	$\beta = 8.0$
OD	-	${}_{oil}\tilde{h}_d = \begin{cases} 43.9\%(\mathrm{Before\,relief}) \\ 14.0\%(\mathrm{After\,relief}) \end{cases}$	-	$\beta = \infty$

Table 5 Condition for maximum response

		BF-VMD	FRVMD	OD
Lv.1	Disp.	Hachinohe	El-Centro	Hachinohe
	Acc.	El-Centro, 5th floor	El-Centro, Base isolation layer	Taft, Base isolation layer
	Share force	Hachinohe	Hachinohe	Hachinohe
Lv.2	Disp.	Art. Kobe	Art. Kobe	Sannomaru
	Acc.	Art. Kobe, Base isolation layer	Art. Taft, Base isolation layer	Art. Kobe, Base isolation layer
	Share force	Art. Taft	Art. Kobe	Sannomaru
Lv.3	Disp.	Takatori	Takatori	Takatori
	Acc.	Takatori, 5th floor	Taft, Base isolation layer	JMA-Kobe, Base isolation layer
	Share force	Takatori	Takatori	Takatori

Figure 6 shows the acceleration time history result of BF-VMD and FRVMD subjected to the artificial wave having the phase property of the 1995 Kobe record. The hysteretic loop depicted in Figure 7 gives single loop when the maximum floor response acceleration is included, that is observed around 10 second. From the time history it is observed that the FRVMD result obtains a lot of high frequency components and larger floor response accelerations compared to the BF-VMD result. The shapes of hysteresis loop between displacement of damping part and viscous damping force for BF-VMD and FRVMD are very similar to each other, although the displacement center of vibrations are different. In contrast, the hysteresis loop between displacement of force restriction part and damping force shows different behavior. The behavior of FRVMD changes sharply when the force restriction is activated, while that of BF-VMD changes slowly. We infer that this difference gives rise to the difference of the floor response acceleration.

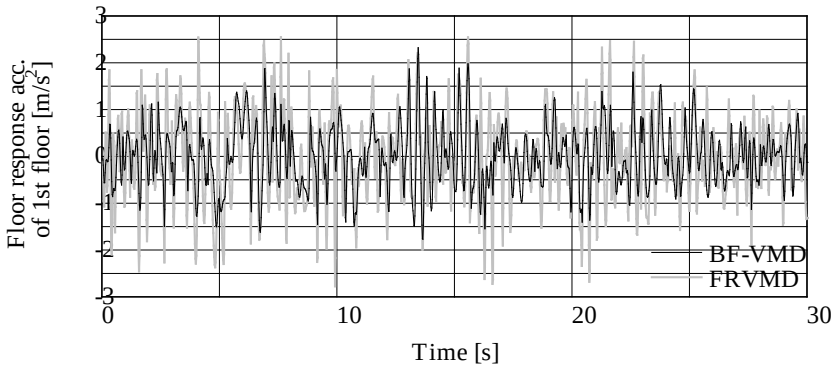

Fig. 6 Acceleration time history for Art. Kobe Earthquake

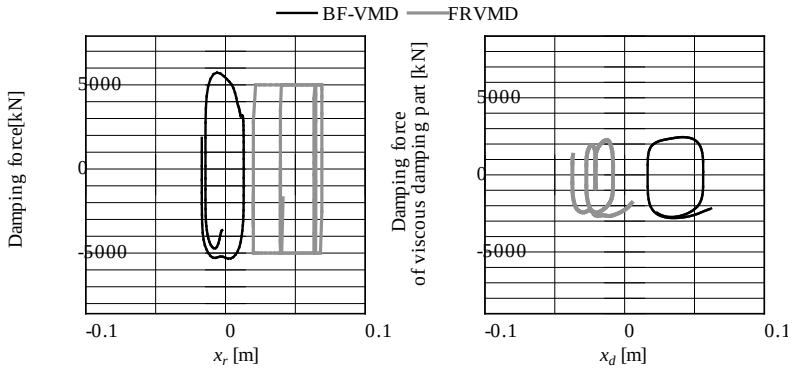

Fig. 7 Hysteresis loop of BF-VMD and FRVMD for the Art. Kobe Earthquake

Figure 8 depicts the amplitude ratio of the 1st floor acceleration to the acceleration of input ground motion in case of Art. Kobe Earthquake. For Both BF-VMD and FRVMD, the amplitude ratio is very small up to 2 Hz. Further increase in frequency results in an increase of the amplitude ratio. Comparing the result of BF-VMD with that of FRVMD, the amplitude ratio of FRVMD is larger than that of BF-VMD especially above 2 Hz. It is found that BF-VMD can keep the floor response acceleration in high frequency range small.

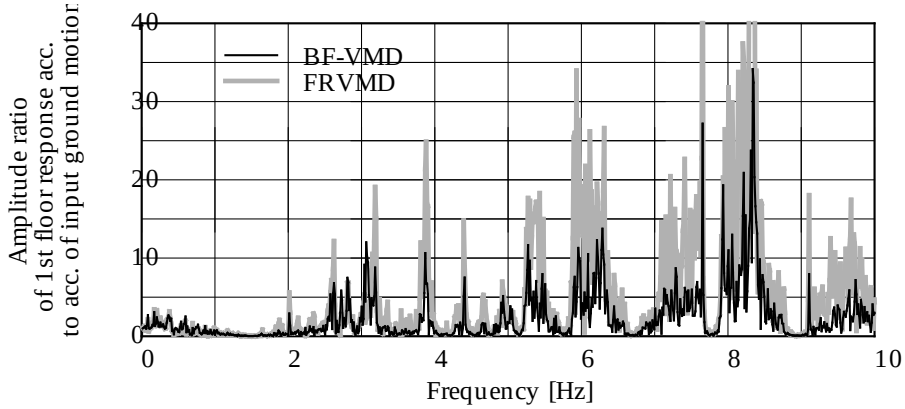

Fig. 8 Amplitude ratio of acceleration for the Art. Kobe Earthquake

4. Conclusion

The viscous mass damper with Bingham fluid origined force restriction mechanism is considered for base isolated structure. Optimum design method is adopted to find four optimum design variables of BF-VMD and the time history analysis results of BF-VMD are compared with that of FRVMD and that of conventional oil dampers. The results indicate that BF-VMD can satisfy the several kinds of design criteria for numbers of input ground motions, while FRVMD and OD cannot satisfy them. Especially BF-VMD can keep the maximum floor response acceleration low compared with FRVMD. It is found that this is because BF-VMD can reduce the floor response acceleration in high frequency range.

5. Acknowledgements

In this study, the simulated ground motion of hypothetical Shin-Tokai Earthquake developed by the Research Consortium of the Chubu Regional Development Bureau, Ministry of Land, Infrastructure, Transport, and Tourism et al. is used.

6. References

[1] Smith, M. C. (2002): Synthesis of Mechanical Networks: the Inerter, IEEE Transactions on Automatic Control, Vol. 47, No. 10, 1648-1662.

[2] Furuhashi, T., Ishimaru, S. (2004) : Mode isolation by inertial mass, Study on response control by inertial mass No.1, J. Struct. Constr. Eng., AIJ, No. 576, 55-62.

[3] Furuhashi, T., Ishimaru, S. (2006) : Response control of multi-degree system by inertial mass, Study on response control by inertial mass No.2, J. Struct. Constr. Eng., AIJ, No. 601, 83-90.

[4] Ishimaru, S., Hata, I., Furuhashi, T. (2011): A simple design method for tuned dynamic mass systems by pseudo mode control, J. Struct. Constr. Eng., AIJ, Vol. 76, No. 661, 509-517.

[5] Kuo, C., Ishimaru, S., Furuhashi, T., Hata, I. (2013): A design method for structures with tuned dynamic mass systems, Response control design of next-generation super high-rise structures against long period waves and pulse wave earthquake ground motions, J. Struct. Constr. Eng., AIJ, Vol. 78, No. 686, 693-702.

[6] Hanzawa, T., Isoda, K. (2009): Experimental study on vertical vibration control by a TMD using a rotating inertia mass, J. Struct. Constr. Eng., AIJ, Vol. 74, No. 640, 1047-1054.

[7] Isoda, K., Hanzawa, T., Tamura, K. (2009): A study on response characteristics of a SDOF model with rotating inertia mass dampers, J. Struct. Constr. Eng., AIJ, Vol. 74, No. 642, 1469-1476.

[8] Isoda, K., Hanzawa, T., Tamura, K. (2010): A study on earthquake energy input to the structure with rotating inertial mass damper, J. Struct. Constr. Eng., AIJ, Vol. 75, No. 650, 751-759.

[9] Isoda, K., Hanzawa, T., Tamura, K. (2013): Basic study on vibration control system by rotating inertial mass dampers concentrated in the lower stories, J. Struct. Constr. Eng., AIJ, Vol. 78, No. 686, 713-722.

[10] Saito, K., Kurita, S., Inoue, N. (2007): Optimum response control of 1-DOF system using linear viscous damper with inertial mass and its kelvin-type modeling, Journal of Structural Engineering, AIJ, Vol.53B, 56-66.

[11] Saito, K., Inoue, N. (2007): A study on optimum response control of passive control systems using viscous damper with inertial mass, Substituting equivalent nonlinear viscous elements for linear viscous elements in optimum control systems, AIJ J. Technol. Des. Vol.13, No.26, 457-462.

[12] Saito, K., Nakaminami, S., Kida, H., Inoue, N. (2008): Vibration tests of 1-story response control system using inertial mass and optimized softy spring and viscous element, Journal of Structural Engineering, AIJ, Vol.54B, 635-648.

[13] Wang, F.-C., et al. (2010): Building suspensions with inerters, Proceedings of the Institution of Mechanical Engineers, Part C Journal of Mechanical Engineering Science, Vol. 224, No. 8, 1605-1616.

[14] Nakaminami, S., Kida, H., Ikago, K., Inoue, N. (2011): Application of viscous mass damper with force restriction mechanism to base-isolated structures and its effectiveness, J. Struct. Constr. Eng., AIJ, Vol. 76, No. 670, 2077-2086.

[15] Nakaminami, S., Kida, H., Ikago, K., Inoue, N. (2014): Effect of damping force restriction and buffer spring of viscous mass damper in base-isolated buildings, J. Struct. Constr. Eng., AIJ, Vol. 79, No. 701, 1055-1064.

[16] Takeshita, M., Ikenaga, M. (2000): Experimental results fundamental tests Binghum material damper, Annual meeting of Architectural Institute of Japan, B-2, 861-862.

[17] Ikenaga, M., Ikago, K., Inoue, N. (2014): Behavior of base-isolated structures using viscous mass damper with force restriction mechanism by Bingham fluid, Annual meeting of Tohoku branch, Architectural Institute of Japan, No.77, 15-18.

[18] J. P. Den Hartog (1985): “Mechanical Vibrations”, 4th ed., Dover, New York.

[19] G.L.Nemhauser, A.H.GRinnooy Kan, M.j.Todd, Editors (1989): Handbooks in Operations Research and Management Science Volume 1 OPTOIMIZATION, North-Holland.